# Analyzing of Delamination in Semirings Attached to Non-Linear Elastic Torsional Springs

Victor Rizov[1*)]

[1*)] Department of Technical Mechanics, University of Architecture, Civil Engineering and Geodesy, 1 Chr. Smirnensky Blvd., 1046 Sofia, Bulgaria, e-mail: v_rizov_fhe@uacg.bg; ORCID: https://orcid.org/0000-0002-0259-3984

http://doi.org/10.29227/IM-2024-02-24

Submission date: *17.04.2024.* | Review date: *14.05.2024*

## Abstract

*The current paper is focused on analysis of delamination of a semiring engineering structure attached to non-linear elastic torsional springs that are situated in the semiring plane. The semiring has arbitrary number of circumferential layers made of non-linear viscoelastic materials that are inhomogeneous along the thickness. The semiring undergoes time-dependent bending rotation at a given cross-section. The delamination is treated from view point of the strain energy release rate (SERR). A methodology for determination of the SERR in semirings attached to torsional springs is worked out on the basis of analysis of the energy balance. The results yielded by this methodology are verified by extracting the SERR from the complementary strain energy. The study presented in the paper provides useful insights into delamination performance of semiring engineering structures which is a premise for enhancing the structural reliability. The effects of various parameters of the semiring geometry, inhomogeneity of layers, non-linear constitutive laws of torsional springs, external loading, number of springs and their locations are examined and clarified.*

**Keywords:** *Semiring structure, Delamination, Torsional springs, Material non-linearity*

## 1. Introduction

Nowadays the components of structures and facilities in various areas of modern engineering are increasingly produced from layered inhomogeneous materials. This can be explained by the fact that the layered materials have shown their remarkable potential as a very good alternative to conventional homogeneous materials like metals. Therefore, the use of layered inhomogeneous structural materials is becoming more and more important [1, 2]. For instance, due to their high strength-to-weight and stiffness-to-weight ratios layered materials are perfect for producing of high-strength and low-weight components of a variety of engineering structures. As a result, both academic circles and industry have concentrated more attention on the studying and application of layered inhomogeneous materials and structures [3, 4].

Delamination in layered components of engineering structures largely affects their performance [5 - 9]. For instance, delamination is one of the reasons for reducing load-bearing capacity. Delamination causes growth of displacements and rotations, and makes layered structures more vulnerable to buckling. Besides, delamination shortens durability of structures and may trigger process of gradual collapse of the structure through increasing of the delamination length. Therefore, it is of crucial importance to analyze and explain the influence of a broad range of factors on delamination behavior in order to improve the performance and increase reliability of layered structures. In this relation, various models with different degree of complexity for studying of delamination behavior have been proposed in the scientific literature in recent decades [5 - 9]. Moreover, there are intrinsic difficulties and many unresolved issues related to delamination. For instance, no enough information about various aspects of the delamination in layered non-linear viscoelastic semirings that are attached to non-linear elastic torsional springs is available.

This issue is treated analytically in the current paper. Delamination of layered non-linear viscoelastic semiring engineering structures that undergo time-dependent bending rotation at a given cross-section is analyzed. The semiring is attached in its ends to short rods. Also, the semiring is attached in two points to non-linear elastic torsional springs located in the semiring plane. The delamination issue is addressed from the SERR point of view. For this purpose, a methodology for determination of the SERR through analyzing the energy balance in semirings attached to torsional springs is elaborated. The SERR is extracted also from the complementary strain energy for verification. Numerical results that give useful insights into the effects of different factors on the SERR are presented in graphical form in the third section of the paper.

## 2. Methodology for Determination of the SERR

The current analysis is concerned with delamination in the semiring engineering structure depicted in Figure 1.

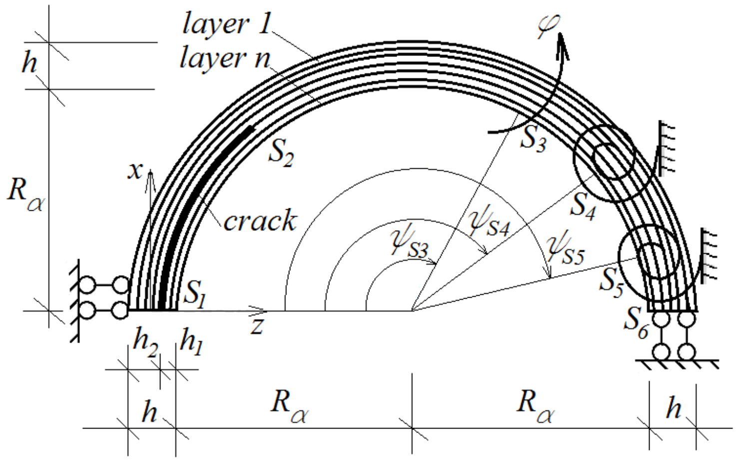

Fig. 1. Semiring structure with a circumferential delamination.

This semiring is built-up by circumferential layers each of them having different material properties and thickness. There is a circumferential delamination crack in portion, $S_1S_2$, of the semiring (Figure 1). The length of the delamination is $a$ . The thicknesses of the internal and external delamination arms are $h_1$ and $h_2$, respectively (Figure 1). The left end of the semiring is attached to two short horizontal rods as depicted in Figure 1. The right end of the semiring is attached to two short vertical rods. Sections, $S_4$ and $S_5$, of the semiring are attached to two non-linear elastic torsional springs. These springs are located in the semiring plane (Figure 1). The semiring undergoes time-dependent rotation in its plane at section, $S_3$ , with law in Eq.(1).

$$\varphi = \theta e^{\lambda t}, \tag{1}$$

where $\varphi$ is the angle of rotation, $t$ is time, $\theta$ and $\lambda$ are parameters.

It is known from the fracture mechanics that the SERR is a widely used parameter when studying delamination. In the present paper, the strain energy release rate, $G$, for the circumferential delamination in the semiring in Figure 1 is obtained by a methodology based on analysis of the energy balance. Equation (2) describes the energy balance when the delamination length increases with $\delta a$ .

$$M_{S3}\delta\varphi + M_{S4}\delta\varphi_{S4} + M_{S5}\delta\varphi_{S5} = \frac{\partial U}{\partial a}\delta a + Gb\delta a, \tag{2}$$

where $M_{S3}$ is the external moment in section, $S_3$, of the semiring, $M_{S4}$ and $M_{S5}$ are the moments in the springs in sections, $S_4$ and $S_5$, respectively, $\varphi_{S4}$ and $\varphi_{S5}$ are the angles of rotation of these sections, $U$ is the strain energy in the semiring, $b$ is the width of the semiring cross-section. By solving Eq. (2) with respect to $G$ , one gets

$$G = \frac{1}{b}\left( M_{S3}\frac{\partial\varphi}{\partial a} + M_{S4}\frac{\partial\varphi_{S4}}{\partial a} + M_{S5}\frac{\partial\varphi_{S5}}{\partial a} - \frac{\partial U}{\partial a} \right). \tag{3}$$

Equation (3) indicates that the angles of rotation, $\varphi$ , $\varphi_{S4}$ and $\varphi_{S5}$ , have to be expressed as functions of the delamination length. For this purpose, applying the integrals of Maxwell-Mohr, one finds that

$$\varphi = \kappa_1 a + \kappa_2\left[\left(R_\alpha + \frac{h}{2}\right)\psi_{S3} - a\right], \tag{4}$$

$$\varphi_{S4} = \kappa_1 a + \kappa_2\left[\left(R_\alpha + \frac{h}{2}\right)\psi_{S3} - a\right] + \kappa_3\left[\left(R_\alpha + \frac{h}{2}\right)(\psi_{S4} - \psi_{S3})\right], \tag{5}$$

$$\varphi_{S5} = \kappa_1 a + \kappa_2\left[\left(R_\alpha + \frac{h}{2}\right)\psi_{S3} - a\right] + \kappa_3\left[\left(R_\alpha + \frac{h}{2}\right)(\psi_{S4} - \psi_{S3})\right] + \kappa_4\left[\left(R_\alpha + \frac{h}{2}\right)(\psi_{S5} - \psi_{S4})\right], \tag{6}$$

where $\kappa_1$ is the change of the curvature of the external delamination arm (this delamination arm has thickness, $h_2$, as depicted in Figure 1), $\kappa_2$, $\kappa_3$ and $\kappa_4$ are the changes of the curvatures of portions, $S_2S_3$, $S_3S_4$ and $S_4S_5$, of the semiring, respectively, $h$ is the thickness of the semiring, the radius, $R_\alpha$, and the central angles, $\psi_{S3}$, $\psi_{S4}$ and $\psi_{S5}$, are defined in Figure 1.

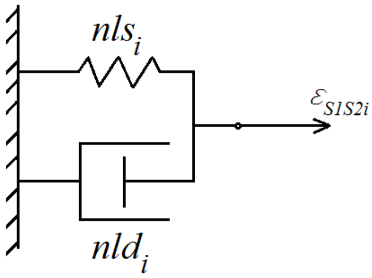

Fig. 2. Viscoelas model.

For determining the changes of the curvatures, one uses Eqs. (7). These equations follow from the fact that the axial forces in the external delamination arm and in the semiring portions are equal to zero.

$$b\sum_{i=1}^{i=n_1}\int_{z_{1i}}^{z_{1i+1}}\sigma_{S1S2i}dz_1 = 0,\quad b\sum_{i=1}^{i=n}\int_{z_{2i}}^{z_{2i+1}}\sigma_{S2S3i}dz_2 = 0,\quad b\sum_{i=1}^{i=n}\int_{z_{3i}}^{z_{3i+1}}\sigma_{S3S4i}dz_3 = 0,\quad b\sum_{i=1}^{i=n}\int_{z_{4i}}^{z_{4i+1}}\sigma_{S4S5i}dz_4 = 0, \quad (7)$$

where $n_1$ and $n$ are the layers in the external delamination arm and in the semiring, respectively, $\sigma_{S1S2i}$ is the stress in the external delamination arm, $\sigma_{S2S3i}$, $\sigma_{S3S4i}$ and $\sigma_{S4S5i}$ are the stresses in portions, $S_2S_3$, $S_3S_4$ and $S_4S_5$, of the semiring, respectively, $z_{1i}$ and $z_{1i+1}$ are the coordinates of the external and the internal surfaces of a layer in the external delamination arm, $z_1$ is the centric axis of the external delamination arm, $z_2$, $z_3$ and $z_4$ are the centric axes of portions, $S_2S_3$, $S_3S_4$ and $S_4S_5$, of the semiring. The internal delamination arm is stresses free (this is due to the fact that section, $S_3$, of the semiring rotates anticlockwise as depicted in Figure 1). Thus, only stresses in the external delamination arm are included in the first equation in (7).

The semiring has non-linear viscoelastic behavior. The stress in the i-th layer of the external delamination arm is related to the strain, $\varepsilon_{S1S2i}$, by the non-linear viscoelastic model depicted in Figure 2. This model has a non-linear spring, $nls_i$, and a non-linear dashpot, $nld_i$. The model is under strain, $\varepsilon_{S1S2i}$, that depends on time according to Eq. (8).

$$\varepsilon_{S1S2i} = \beta e^{\lambda t}, \quad (8)$$

where $\beta$ is a parameter. Eq. (9) describes the non-linear stress-strain constitutive law of the spring [10].

$$\sigma_{nlsi} = \frac{\varepsilon_{S1S2i}}{L_i + Q_i\varepsilon_{S1S2i}}, \quad (9)$$

where $\sigma_{nlsi}$ is the stress in the spring, $L_i$ and $Q_i$ are material properties. The behavior of the dashpot follows the non-linear constitutive law in Eq. (10) [10].

$$\sigma_{nldi} = \frac{\dot{\varepsilon}_{S1S2i}}{B_i + D_i\dot{\varepsilon}_{S1S2i}}, \quad (10)$$

where $\dot{\varepsilon}_{S1S2i}$ is the first derivative of the strain with respect to time, $B_i$ and $D_i$ are material properties. By inserting of (8) in (10), one gets

$$\sigma_{nldi} = \frac{\beta\lambda e^{\lambda t}}{B_i + D_i\beta\lambda e^{\lambda t}}. \quad (11)$$

Eq. (12) describes the stress in the model in Figure 2.

$$\sigma_{S1S2i} = \sigma_{nlsi} + \sigma_{nldi}. \quad (12)$$

Applying Eqs. (9), (11) and (12), one has

$$\sigma_{S1S2i} = \frac{\varepsilon_{S1S2i}}{L_i + Q_i \varepsilon_{S1S2i}} + \frac{\beta \lambda e^{\lambda t}}{B_i + D_i \beta \lambda e^{\lambda t}}. \tag{13}$$

Eq. (13) is the non-linear stress-strain-time relationship for the i-th layer in the external delamination arm. The strain, $\varepsilon_{S1S2i}$, changes along the thickness of the external crack arm according to the law in Eq. (14).

$$\varepsilon_{S1S2i} = \kappa_1 \left( z_1 - z_{1n} \right), \tag{14}$$

where $z_{1n}$ is the coordinate of the neutral axis. Inserting of (14) in (13), one gets

$$\sigma_{S1S2i} = \frac{\kappa_1 \left( z_1 - z_{1n} \right)}{L_i + Q_i \kappa_1 \left( z_1 - z_{1n} \right)} + \frac{\beta \lambda e^{\lambda t}}{B_i + D_i \beta \lambda e^{\lambda t}}. \tag{15}$$

The materials of the semiring layers are continuously inhomogeneous along the thickness. Eqs. (16) describe the change of material properties, $L_i$, $Q_i$, $B_i$ and $D_i$, across the i-th layer thickness.

$$L_i = L_{iext} e^{\delta_i \frac{z_1 - z_{1i}}{z_{1i+1} - z_{1i}}},\quad Q_i = Q_{iext} e^{\eta_i \frac{z_1 - z_{1i}}{z_{1i+1} - z_{1i}}},\quad B_i = B_{iext} e^{\mu_i \frac{z_1 - z_{1i}}{z_{1i+1} - z_{1i}}},\quad D_i = D_{iext} e^{\omega_i \frac{z_1 - z_{1i}}{z_{1i+1} - z_{1i}}}, \tag{16}$$

where $L_{iext}$, $Q_{iext}$, $B_{iext}$ and $D_{iext}$ are the values of $L_i$, $Q_i$, $B_i$ and $D_i$ at the external surface of the layer, $\delta_i$, $\eta_i$, $\mu_i$ and $\omega_i$ are parameters.

The stress in portion, $S_2S_3$, of the semiring is expressed by replacing $\kappa_1$, $z_1$ and $z_{1n}$ with $\kappa_2$, $z_2$ and $z_{2n}$ in Eq. (15), i.e.

$$\sigma_{S2S3i} = \frac{\kappa_2 \left( z_2 - z_{2n} \right)}{L_i + Q_i \kappa_2 \left( z_2 - z_{2n} \right)} + \frac{\beta \lambda e^{\lambda t}}{B_i + D_i \beta \lambda e^{\lambda t}}. \tag{17}$$

In analogical manner, the stresses in the i-th layer of portions, $S_3S_4$ and $S_4S_5$, of the semiring are obtained as

$$\sigma_{S3S4i} = \frac{\kappa_3 \left( z_3 - z_{3n} \right)}{L_i + Q_i \kappa_3 \left( z_3 - z_{3n} \right)} + \frac{\beta \lambda e^{\lambda t}}{B_i + D_i \beta \lambda e^{\lambda t}},\quad \sigma_{S4S4i} = \frac{\kappa_4 \left( z_4 - z_{4n} \right)}{L_i + Q_i \kappa_4 \left( z_4 - z_{4n} \right)} + \frac{\beta \lambda e^{\lambda t}}{B_i + D_i \beta \lambda e^{\lambda t}}. \tag{18}$$

There are 8 unknown parameters, $\kappa_1$, $\kappa_2$, $\kappa_3$, $\kappa_4$, $z_{1n}$, $z_{2n}$, $z_{3n}$ and $z_{4n}$, in dependences (15), (17), and (18). Therefore, Eqs. (7) have to be complemented with a further 4 equations. Applying the equation of moment equilibrium for sections, $S_2$, $S_4$ and $S_5$, of the semiring, one gets

$$b \sum_{i=1}^{i=n_1} \int_{z_{1i}}^{z_{1i+1}} \sigma_{S1S2i} z_1 dz_1 + b \sum_{i=1}^{i=n} \int_{z_{2i}}^{z_{2i+1}} \sigma_{S2S3i} z_2 dz_2 = 0,\quad b \sum_{i=1}^{i=n} \int_{z_{3i}}^{z_{3i+1}} \sigma_{S3S4i} z_3 dz_3 + b \sum_{i=1}^{i=n} \int_{z_{4i}}^{z_{4i+1}} \sigma_{S4S5i} z_4 dz_4 = M_{S4} \tag{19}$$

$$b \sum_{i=1}^{i=n} \int_{z_{4i}}^{z_{4i+1}} \sigma_{S4S5i} z_4 dz_4 + b \sum_{i=1}^{i=n} \int_{z_{5i}}^{z_{5i+1}} \sigma_{S5S6i} z_5 dz_5 = M_{S5}, \tag{20}$$

where the stress, $\sigma_{S5S6i}$, in the i-th layer of portion, $S_5S_6$, of the semiring is

$$\sigma_{S5S6i} = \frac{\kappa_5 \left( z_5 - z_{5n} \right)}{L_i + Q_i \kappa_5 \left( z_5 - z_{5n} \right)} + \frac{\beta \lambda e^{\lambda t}}{B_i + D_i \beta \lambda e^{\lambda t}}. \tag{21}$$

The moments, $M_{S4}$ and $M_{S5}$, in the non-linear elastic springs in sections, $S_4$ and $S_5$, of the semiring that are involved in Eqs. (19) and (20) are determined by the following non-linear constitutive laws [6]:

$$M_{S4} = H_{S4}\left[1-\left(1-\frac{\varphi_{S4}}{T_{S4}}\right)^{f_{S4}}\right],\quad M_{S5} = H_{S5}\left[1-\left(1-\frac{\varphi_{S5}}{T_{S5}}\right)^{f_{S5}}\right], \tag{22}$$

where $H_{S4}$, $H_{S5}$, $T_{S4}$, $T_{S5}$, $f_{S4}$ and $f_{S5}$ are parameters of the springs, the angles of rotation, $\varphi_{S4}$ and $\varphi_{S5}$, of sections, $S_4$ and $S_5$, are obtained by Eqs. (5) and (6), respectively.

Equation (21) indicates that a further two unknowns, $k_5$ and $z_{5n}$, are involved in Eq. (20). Therefore, Eqs. (7) and (20) are supplemented with a further two equations which are constituted in the following manner. The fact that the axial force in portion, $S_5S_6$, of the semiring is zero leads to Eq. (23).

$$b\sum_{i=1}^{i=n}\int_{z_{5i}}^{z_{5i+1}}\sigma_{S5S6i}dz_5 = 0 . \tag{23}$$

Equation (24) is written by using the fact that the rotation, $\varphi_{S6}$, of section, $S_6$, of the semiring is zero.

$$\varphi_{S6} = \kappa_1 a + \kappa_2\left[\left(R_\alpha+\frac{h}{2}\right)\psi_{S3} - a\right] + \kappa_3\left[\left(R_\alpha+\frac{h}{2}\right)(\psi_{S4}-\psi_{S3})\right] +$$
$$+\kappa_4\left[\left(R_\alpha+\frac{h}{2}\right)(\psi_{S5}-\psi_{S4})\right] + \kappa_5\left[\left(R_\alpha+\frac{h}{2}\right)(\pi-\psi_{S5})\right] . \tag{24}$$

It should be noted that Eq. (24) is composed by expressing the rotation of section, $S_6$, with the help of the integrals of Maxwell-Mohr.

Equations (7), (19), (20), (23) and (24) together with Eq. (4) (it should be mentioned here that Eq. (4) can be treated as equation with unknowns, $\kappa_1$ and $\kappa_2$, since the law for variation of $\varphi$ is given (refer to Eq. (1)) are solved with respect to $\kappa_1$, $\kappa_2$, $\kappa_3$, $\kappa_4$, $\kappa_5$, $z_{1n}$, $z_{2n}$, $z_{3n}$, $z_{4n}$ and $z_{5n}$ by the MatLab.

The external moment, $M_{S3}$, in section, $S_3$, of the semiring that is involved in Eq. (3) is determined by Eq. (25) which is constituted by applying the equation of moment equilibrium for section, $S_3$.

$$b\sum_{i=1}^{i=n}\int_{z_{2i}}^{z_{2i+1}}\sigma_{S2S3i}z_2dz_2 + b\sum_{i=1}^{i=n}\int_{z_{3i}}^{z_{3i+1}}\sigma_{S3S4i}z_3dz_3 + M_{S3} = 0 . \tag{25}$$

Equation (26) is used for obtaining the strain energy, $U$, that is involved in (3).

$$U = ab\sum_{i=1}^{i=n_1}\int_{z_{1i}}^{z_{1i+1}}u_{0S1S2i}dz_1 + \left[\left(R_\alpha+\frac{h}{2}\right)\psi_{S3}-a\right]b\sum_{i=1}^{i=n}\int_{z_{2i}}^{z_{2i+1}}u_{0S2S3i}dz_3 +$$
$$\left[\left(R_\alpha+\frac{h}{2}\right)(\psi_{S4}-\psi_{S3})\right]b\sum_{i=1}^{i=n}\int_{z_{3i}}^{z_{3i+1}}u_{0S3S4i}dz_4 + \left[\left(R_\alpha+\frac{h}{2}\right)(\psi_{S5}-\psi_{S4})\right]b\sum_{i=1}^{i=n}\int_{z_{4i}}^{z_{4i+1}}u_{0S4S5i}z_4dz_4 +$$
$$\left[\left(R_\alpha+\frac{h}{2}\right)(\pi-\psi_{S5})\right]b\sum_{i=1}^{i=n}\int_{z_{5i}}^{z_{5i+1}}u_{0S5S6i}dz_5 , \tag{26}$$

where $u_{0S1S2i}$ is the specific strain energy in the external delamination arm, $u_{0S2S3i}$, $u_{0S3S4i}$, $u_{0S4S5i}$ and $u_{0S5S6i}$ are the specific strain energies in the portions, $S_2S_3$, $S_3S_4$, $S_4S_5$ and $S_5S_6$, of the semiring, respectively. Eq. (27) is used for obtaining of $u_{0S1S2i}$, i.e.

$$u_{0S1S2i} = \int_0^{\varepsilon_{S1S2i}} \sigma_{S1S2i} d\varepsilon_{S1S2i} \quad . \tag{27}$$

The specific strain energy in the portion, $S_2S_3$, of the semiring, is determined by replacing of $\sigma_{S1S2i}$ and $\varepsilon_{S1S2i}$ with $\sigma_{S2S3i}$ and $\varepsilon_{S2S3i}$ in Eq. (27). The specific strain energies in portions, $S_3S_4$, $S_4S_5$ and $S_5S_6$, of the semiring are derived by performing analogical replacements in Eq. (27).

At the end, the SERR is derived by inserting $M_{S3}$, $M_{S4}$, $M_{S5}$, $\varphi$, $\varphi_{S4}$, $\varphi_{S5}$ and $U$ in Eq. (3).

A check-up of the SERR is carried-out by applying an approach that extracts $G$ from the complementary strain energy [9]. This approach results in Eq. (28).

$$G = \frac{U^*_{S1S2} - U^*_{S2S3}}{b} \quad , \tag{28}$$

where

$$U^*_{S1S2} = \sum_{i=1}^{i=n_1} \int_{z_{1i}}^{z_{1i+1}} u^*_{0S1S2i}\, dz_1 \quad , \quad U^*_{S2S3} = \sum_{i=1}^{i=n} \int_{z_{2i}}^{z_{2i+1}} u^*_{0S2S3i} dz_2 \quad 0 \quad , \tag{29}$$

$$u^*_{0S1S2i} = \sigma_{S1S2i}\varepsilon_{S1S2i} - \int_0^{\varepsilon_{S1S2i}} \sigma_{S1S2i} d\varepsilon_{S1S2i} \quad , \quad u^*_{0S2S3i} = \sigma_{S2S3i}\varepsilon_{S2S3i} - \int_0^{\varepsilon_{S2S3i}} \sigma_{S2S3i} d\varepsilon_{S2S3i} \quad . \tag{30}$$

The SERR found by Eq. (28) matches that derived by Eq. (3).

**3. Numerical Results**

Results of the SERR analysis are given in Figures 3, 4 and 5 for a layered viscoelastic semiring structure with $n_1 = 3$, $n = 5$, $h = 0.008$ m, $R_\alpha = 0.300$ m, $\psi_{S3} = 5\pi/8$, $\psi_{S4} = 6\pi/8$ and $\psi_{S5} = 7\pi/8$. The plots in Figures 3, 4 and 5 give an indication for the change of SERR induced by alteration of various parameters.

Figure 3 gives plots of the non-dimensional SERR against the parameter, $\delta_1$, for different values of the parameter, $\theta$. One can see in Figure 3 that the non-dimensional SERR rises when the value of $\delta_1$ increases (this behavior is related to the decay of the semiring stiffness). Comparison of the three plots in Figure 3 shows that the non-dimensional SERR is highly sensitive towards the value of $\theta$. Rise of $\theta$ induces rise of the non-dimensional SERR (this observation is related to the rise of the angle of rotation of section, $S_3$, of the semiring structure).

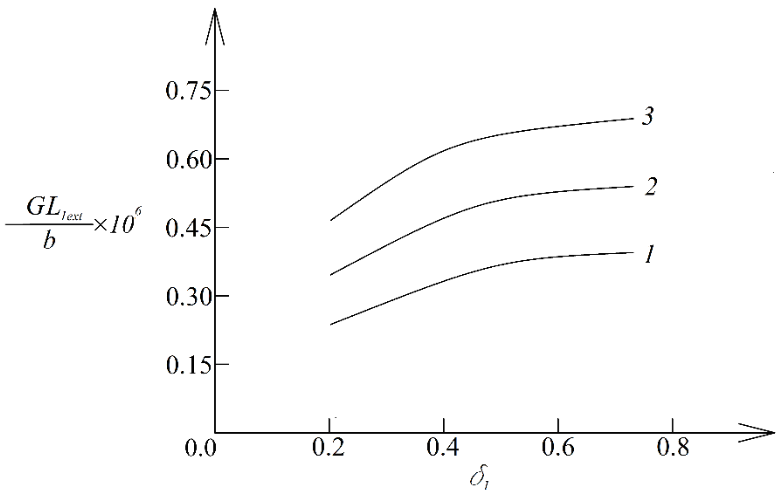


Fig. 3. Dependence of the non-dimensional SERR on the parameter $\delta_1$ (curve 1 – at $\theta = 0.003$ rad, curve 2 – at $\theta = 0.006$ rad and curve 3 – at $\theta = 0.009$ rad).

Figure 4 shows results for the non-dimensional SERR obtained by varying $H_{S5} / H_{S4}$ ratio.

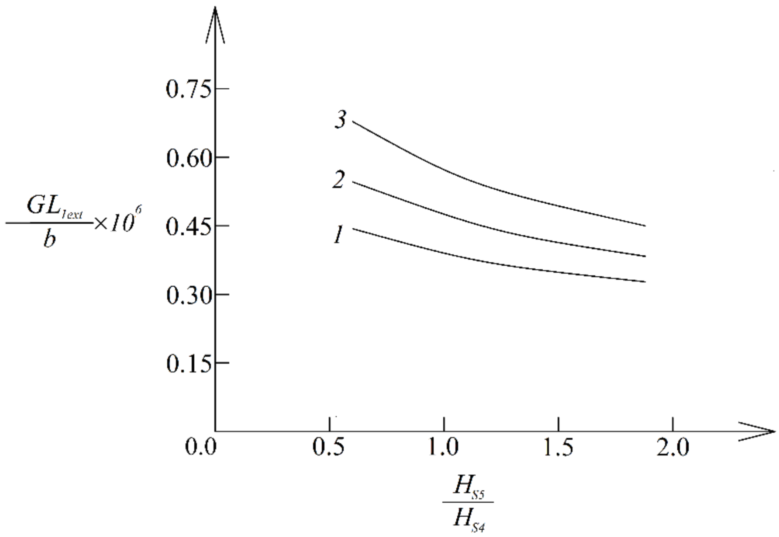


Fig. 4. Dependence of the non-dimensional SERR on $H_{S5} / H_{S4}$ ratio (curve 1 – at $\mu_1 = 0.2$, curve 2 – at $\mu_1 = 0.4$ and curve 3 – at $\mu_1 = 0.6$).

One can observe in Figure 4 that the non-dimensional SERR continuously reduces when $H_{S5} / H_{S4}$ ratio rises. The plots in Figure 4 illustrate also the influence of the parameter, $\mu_1$, on the non-dimensional SERR. The rise of the non-dimensional SERR when $\mu_1$ grows is related to reduction of the stiffness of the semiring (Figure 4).

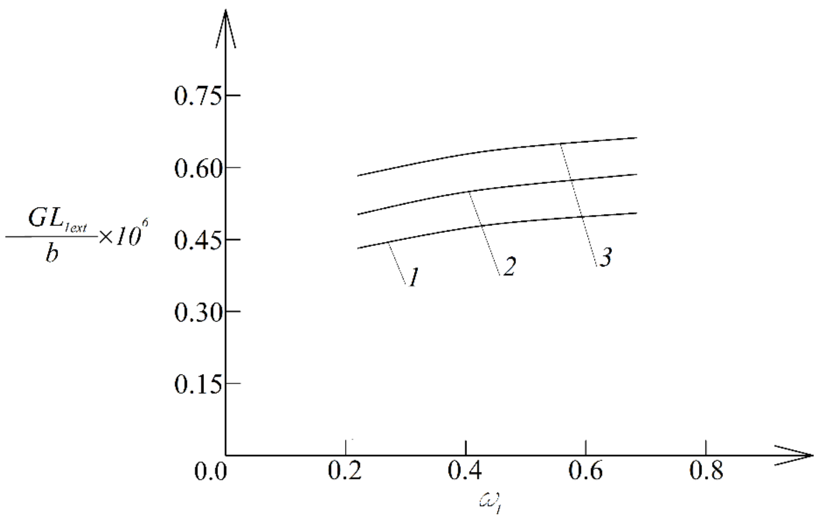


Fig. 5. Dependence of the non-dimensional SERR on the parameter $\omega_1$ (curve 1 – at $\eta_1 = 0.3$, curve 2 – at $\eta_1 = 0.6$ and curve 3 – at $\eta_1 = 0.9$).

The change of the non-dimensional SERR due to rise of the parameter, $\omega_1$, is also analyzed. The results yielded by the analysis are illustrated by the plots given in Figure 5. The analysis predicts rise of the non-dimensional SERR when the value of $\omega_1$ increases (Figure 5). The influence of the parameter, $\eta_1$, is analyzed too. The results of the analysis indicate rise of the non-dimensional SERR with rise of $\eta_1$ as shown in Figure 5.

**4. Conclusion**

The behavior of a semiring engineering structure with a circumferential delamination is determined. The semiring is built-up by circumferential layers made of non-linear viscoelastic materials. The semiring is attached to two non-linear elastic torsional springs. Also, the semiring is attached to short rods in its ends. The semiring undergoes bending rotation at a given section with a time-dependent law. The SERR is determined by a methodology based on analysis of the energy balance and verified by extracting it from the complementary strain energy. It is shown that for the semiring under consideration the SERR rises when the value of $\delta_1$ increases. Rise of $\theta$ also induces rise of the SERR. The analysis detects reduction of the SERR when $H_{S5}/H_{S4}$ ratio rises. Rise of the SERR is observed when $\mu_1$ grows. The SERR grows when the value of $\omega_1$ increases. Rise of $\eta_1$ generates increase of SERR. It can be generalized that the present research enhances understanding of the delamination behavior of semirings attached to non-linear elastic torsional springs. The methodology presented here is usable also for analyzing delamination in semirings attached to more than two non-linear elastic torsional springs.

**References**


1. Sy-NgocNguyen, JaehunLee, Jang-Woo Han and Maenghyo Cho, "A coupled hygrothermo-mechanical viscoelastic analysis of multilayered composite plates for long-term creep behaviors", Composite Structures, 242, pp. 112030 (2020).
2. Y. Tokovyy and C.C. Ma, "Elastic Analysis of Inhomogeneous Solids: History and Development in Brief", Journal of Mechanics, 18, pp. 1-14 (2019).
3. R. M. Mahamood and E.T. Akinlabi, Functionally Graded Materials (Springer, 2017).
4. S. Shrikantha Rao and K.V. Gangadharan, "Functionally graded composite materials: an overview", Procedia Materials Science, 5, pp. 1291-1299 (2014).
5. J. W. Hutchinson and Z. Suo, "Mixed mode cracking in layered materials", Adv. Appl. Mech. 64, pp. 804 – 810 (1992).
6. N. E. Dowling, Mechanical behavior of materials (Person, 2013).
7. N. A. Dolgov, "Determination of Stresses in a Two-Layer Coating", Strength of Materials, 37, pp. 422-431 (2005).
8. V. Rizov, "Influence of the viscoelastic material behavior on the delamination in multilayered beam", Procedia Structural Integrity, 25, pp. 88–100 (2020).
9. V. Rizov, "Longitudinal fracture of functionally graded beams with non-linear rheological behaviour", Procedia Structural Integrity, 54, pp. 468–474 (2024).
10. P. A. Lukash, Fundamentals of Non-linear Structural Mechanics (Stroiizdat, 1978).